

# Charm production and energy loss at the LHC with ALICE

A. DAINESE

*Università degli Studi di Padova and INFN, via Marzolo 8, 35131 Padova, Italy*

for the ALICE Collaboration

Received 29 September 2004;  
final version 29 September 2004

The latest results on the ALICE performance for production and in-medium QCD energy loss measurements of charm particles at the LHC are presented.

*PACS:* 25.75.-q, 14.65.Dw, 13.25.Ft

*Key words:* pp and Pb–Pb collisions, charm production, heavy-quark QCD energy loss

## 1 Introduction

The ALICE experiment [1] will study proton–proton (pp), proton–nucleus (pA) and nucleus–nucleus (AA) collisions at the LHC, with centre-of-mass energies per nucleon–nucleon (NN) pair,  $\sqrt{s_{NN}}$ , from 5.5 TeV (for Pb–Pb) to 14 TeV (for pp).

ALICE is the dedicated heavy-ion experiment at the LHC and its primary physics goal is the investigation of the properties of QCD matter at the energy densities of several hundred times the density of atomic nuclei that will be reached in central Pb–Pb collisions. In these conditions a deconfined state of quarks and gluons, the Quark–Gluon Plasma (QGP), is expected to be formed [2]. As we shall detail in the following Section 2, heavy quarks, and hard partons in general, probe this medium via the mechanism of QCD energy loss [2, 3]. An estimate of the medium-induced suppression of open charm mesons is presented in Section 4, along with the expected ALICE sensitivity for the measurement of this effect.

The unique features of the ALICE detector, such as the low-momentum acceptance and the excellent particle identification, will also allow a rich program of pp physics, complementary to the those of ATLAS, CMS and LHCb. One outstanding example is the measurement of the charm production cross section, which is described in Section 3.

## 2 Heavy-quark production and energy loss

Heavy quarks are produced in primary partonic scatterings with large virtuality  $Q$  (momentum transfer) and, thus, on short temporal and spatial scales,  $\Delta\tau \sim \Delta r \sim 1/Q$ . In fact, the minimum virtuality  $Q_{\min} = 2m_Q$  in the production of a  $Q\bar{Q}$  pair implies a space-time scale of  $\sim 1/(2m_Q) \simeq 1/2.4 \text{ GeV}^{-1} \simeq 0.1 \text{ fm}$  (for charm). Therefore, in nucleus–nucleus collisions, the hard production process itself should not be affected by the successive formation of the high-density deconfined medium.

Given the large virtualities that characterize the production of heavy quarks,

the cross sections in nucleon–nucleon collisions can be calculated in the framework of collinear factorization and perturbative QCD (pQCD). The inclusive differential  $Q\bar{Q}$  cross section is written as:

$$d\sigma_{\text{NN}\rightarrow Q\bar{Q}X}(\sqrt{s_{\text{NN}}}, m_Q, \mu_R^2, \mu_F^2) = \sum_{i,j=q,\bar{q},g} f_i(x_1, \mu_F^2) \otimes f_j(x_2, \mu_F^2) \otimes d\hat{\sigma}_{ij\rightarrow Q\bar{Q}\{k\}}(\alpha_s(\mu_R^2), \mu_F^2, m_Q, x_1, x_2), \quad (1)$$

where  $d\hat{\sigma}_{ij\rightarrow Q\bar{Q}\{k\}}$  is the perturbative partonic hard part, calculable as a power series in the strong coupling  $\alpha_s(\mu_R^2)$ , which depends on the renormalization scale  $\mu_R$ ; currently, calculations are performed up to next-to-leading order (NLO),  $\mathcal{O}(\alpha_s^3)$ . The nucleon Parton Distribution Functions (PDFs) for each parton  $i(j)$  at momentum fraction  $x_1(x_2)$  and factorization scale  $\mu_F$ , which can be interpreted as the virtuality of the hard process, are denoted by  $f_i(x, \mu_F^2)$ . At LHC energies, there are large uncertainties, of about a factor 2, on the charm and beauty production cross sections, estimated by varying the values of the masses and of the scales  $\mu_F$  and  $\mu_R$  (much smaller uncertainties,  $\approx 20\%$ , arise from the indetermination in the PDFs) [4, 5]. Different predictions for the D-meson cross section as a function of the transverse momentum ( $p_t$ ) will be shown in Section 3, along with the ALICE capability to constrain the pQCD parameter space for charm production.

For hard processes such as heavy-quark production, in the absence of nuclear and medium effects, a nucleus–nucleus collision would behave as a superposition of independent NN collisions. The hard processes yields would then scale from pp to AA proportionally to the number of inelastic NN collisions (binary scaling). Applying binary scaling to ‘average’ pQCD results and taking into account nuclear shadowing effects —the PDF suppression at small  $x$  in the nucleus— we expect about 115  $c\bar{c}$  and about 5  $b\bar{b}$  pairs per central (5%  $\sigma^{\text{tot}}$ ) Pb–Pb collision at  $\sqrt{s_{\text{NN}}} = 5.5$  TeV (these numbers are obtained at NLO using the HVQMNR program [6] with  $m_c = 1.2$  GeV and  $\mu_F = \mu_R = 2\mu_0$  for charm and  $m_b = 4.75$  GeV and  $\mu_F = \mu_R = \mu_0$  for beauty, where  $\mu_0^2 \equiv m_Q^2 + (p_{t,Q}^2 + p_{t,\bar{Q}}^2)/2$ ; the PDF set is CTEQ 4M [7] corrected for nuclear shadowing according to the EKS98 parameterization [8]).

Deviations from binary scaling correspond to deviations from unity of the *nuclear modification factor* (here defined for D mesons):

$$R_{\text{AA}}^{\text{D}}(p_t) \equiv \frac{1}{\text{binary NN collisions}} \times \frac{dN_{\text{AA}}^{\text{D}}/dp_t}{dN_{\text{pp}}^{\text{D}}/dp_t}. \quad (2)$$

Note that at the LHC, pp and Pb–Pb collisions will be run at different energies and an extrapolation of the measured pp yields will have to be applied to define  $R_{\text{AA}}$ . Such extrapolation can be reliably done by means of pQCD, since it was shown [4] that the ratios of calculation results at different  $\sqrt{s}$  are basically insensitive to the choice of masses and scales.

Experiments at the Relativistic Heavy-Ion Collider (RHIC) have shown that the nuclear modification factor is a powerful tool for the study of the interaction of the produced hard partons with the medium formed in the collision. The suppression

of a factor 4–5 of  $R_{AA}$  for charged hadrons and neutral pions for  $p_t \gtrsim 5$  GeV/ $c$  observed in central Au–Au collisions at  $\sqrt{s_{NN}} = 130$ –200 GeV is interpreted as a consequence of parton energy loss in a dense medium [9].

An intense theoretical activity has developed around the subject of parton energy loss via medium-induced gluon radiation [10–13]. In our sensitivity studies (see Section 4) we have considered the BDMPS model in the multiple soft scattering approximation [11]. Its main features are summarized in the functional form of the average energy loss for a high-energy ( $E \rightarrow \infty$ ) hard parton with path length  $L$  in the medium:

$$\langle \Delta E \rangle \propto \alpha_s C_R \hat{q} L^2. \quad (3)$$

$C_R$  is the Casimir coupling factor (3 if the considered hard parton is a gluon, 4/3 if it is a quark);  $\hat{q}$  is the transport coefficient of the medium, defined as the average transverse momentum squared transferred to the projectile per unit mean free path and it is proportional to the density of scattering centres (gluons) in the medium and to the typical momenta exchanged in interactions with such centres; the characteristic  $L^2$ -dependence arises from the non-Abelian nature of QCD. The average energy loss is independent of the initial parton energy  $E$ , if this is very large. In the more realistic case of parton energies of  $\sim 10$ –50 GeV, there is an intrinsic dependence of the radiated energy on the initial energy, determined by the fact that the former cannot be larger than the latter,  $\Delta E \leq E$ . A rigorous theoretical treatment of this finite-energy constraint is at present lacking in the BDMPS framework and approximations have to be adopted, which introduce uncertainties in the results [14].

Due to the large values of their masses the charm and beauty quarks are qualitatively different probes from light partons. Heavy quarks with momenta up to 40–50 GeV/ $c$  propagate with a velocity significantly lower than the velocity of light. As a consequence gluon radiation at angles  $\Theta$  smaller than their mass-to-energy ratio  $\Theta_0 = m_Q/E_Q$  is suppressed by destructive interference [15]. The relatively depopulated cone around the heavy-quark direction with  $\Theta < \Theta_0$  is called ‘dead cone’. In Ref. [16], on the basis of an approximation of the dead-cone effect, charm quarks were predicted to lose much less energy than light quarks. A recent detailed calculation [17] confirms this qualitative feature, although the effect is found to be quantitatively smaller than in Ref. [16].

At the LHC, the abundant production of charm quarks will allow to study the mass dependence of parton quenching and, thus, to test experimentally these effects.

### 3 Measurement of open charm production with ALICE

One of the most promising channels for open charm detection is the  $D^0 \rightarrow K^- \pi^+$  decay (and its charge conjugate), which has a branching ratio ( $BR$ ) of about 3.8%. The expected production yields per unit of rapidity,  $y$ , at central rapidity for  $D^0$  (and  $\bar{D}^0$ ) mesons decaying in a  $K^\mp \pi^\pm$  pair, estimated [5] on the basis of NLO pQCD calculations, are  $BR \times dN/dy = 5.3 \times 10^{-1}$  in central (5%  $\sigma^{\text{tot}}$ ) Pb–Pb collisions at

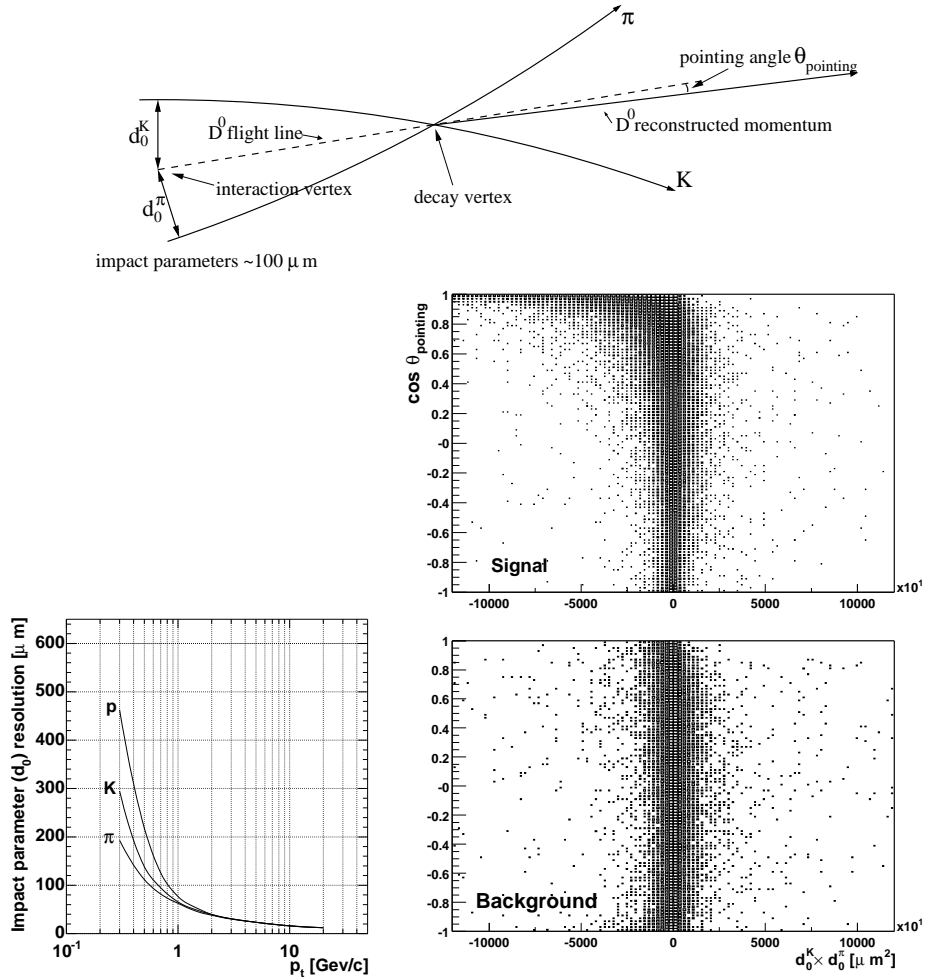


Fig. 1. Top: sketch of the  $D^0 \rightarrow K^- \pi^+$  decay. Bottom-left:  $p_t$ -dependence of the track impact-parameter resolution in central Pb–Pb collisions with the ALICE detector, for  $\pi^\pm$ ,  $K^\pm$  and  $p/\bar{p}$ . Bottom-right: correlation between the cosine of the pointing angle and the product of the impact parameters for signal and background  $D^0 \rightarrow K^- \pi^+$  candidates.

$\sqrt{s_{\text{NN}}} = 5.5 \text{ TeV}$  and  $BR \times dN/dy = 7.5 \times 10^{-4}$  in pp collisions at  $\sqrt{s} = 14 \text{ TeV}$ .

Figure 1 (top) shows a sketch of the decay: the main feature of this topology is the presence of two tracks with impact parameters<sup>1)</sup>  $d_0 \simeq 100 \mu\text{m}$  (the mean proper decay length of  $D^0$  mesons is  $c\tau \simeq 124 \mu\text{m}$ ). Excellent tracking and vertex-

<sup>1)</sup> We define as impact parameter,  $d_0$ , the distance of closest approach of the track to the interaction vertex, in the plane transverse to the beam direction (see sketch in Fig. 1).

ing capabilities are necessary to extract the signal out of the huge combinatorial background in central Pb–Pb collisions, where up to several thousand charged particles might be produced per unit of rapidity (simulations were performed with  $dN_{\text{charged}}/dy = 6000$ ).

The barrel tracking system of ALICE, composed of the Inner Tracking System (ITS), the Time Projection Chamber (TPC) and the Transition Radiation Detector (TRD), embedded in a magnetic field of 0.5 T, allows track reconstruction in the pseudorapidity range  $-0.9 < \eta < 0.9$  with a momentum resolution better than 2% for  $p_t < 10$  GeV/ $c$  and an impact-parameter resolution (shown in the bottom-left panel of Fig. 1) better than 60  $\mu\text{m}$  for  $p_t > 1$  GeV/ $c$ , mainly provided by the two layers, at  $r = 4$  and 7 cm, of silicon pixel detectors of the ITS.

The detection strategy [18] to cope with the large combinatorial background from the underlying event is based on the selection of displaced-vertex topologies. The impact parameter  $d_0$  is given a sign according to the position of the track with respect to the main interaction vertex, so that well-separated signal topologies have impact parameters,  $d_0^K$  and  $d_0^\pi$ , large and with opposite signs. Therefore, the product of the impact parameters is required to be negative and large in absolute value, e.g.  $d_0^K \times d_0^\pi < -2 \times 10^4 \mu\text{m}^2$ . Another suitable variable is the pointing angle  $\theta_{\text{pointing}}$  between the reconstructed  $D^0$  momentum and its flight-line (see sketch in Fig. 1), which is required to be close to zero, e.g.  $\cos \theta_{\text{pointing}} > 0.98$ . We found that these two variables are strongly correlated for the signal and uncorrelated for the background combinations (see bottom-right panel of Fig. 1); therefore, their simultaneous use is extremely efficient in increasing the signal-to-background ratio. After such selection, a standard invariant-mass analysis can be used to extract the amount of signal. The strategy was optimized separately for pp and Pb–Pb collisions, as a function of the  $D^0$  transverse momentum [19]. The requirement of K tagging for one of the two tracks in the high-resolution Time-Of-Flight (TOF) detector and the low value of the magnetic field allow to extend the  $D^0$  signal extraction down to almost zero transverse momentum.

The expected performance for central Pb–Pb (5%  $\sigma^{\text{tot}}$ ) and for pp collisions is summarized in Fig. 2. The accessible  $p_t$  range is 1–14 GeV/ $c$  for Pb–Pb and 0.5–14 GeV/ $c$  for pp. The statistical error corresponding to 1 month of Pb–Pb data-taking ( $\sim 10^7$  central events) and 9 months of pp data-taking ( $\sim 10^9$  events) is better than 15–20% and the systematic error (acceptance and efficiency corrections, subtraction of the feed-down from  $B \rightarrow D^0 + X$  decays, cross-section normalization, centrality selection for Pb–Pb) is better than 20% [19].

On the right-hand panel of Fig. 2 the expected sensitivity of ALICE for the measurement of the  $D^0$   $p_t$ -differential cross section is compared to the uncertainty of pQCD calculations that we mentioned in Section 2. The  $d^2\sigma^{D^0}/dp_t dy$  curves shown in the figure were obtained by applying the PYTHIA [20] fragmentation model to c-quark  $p_t$  distributions calculated at NLO with the HVQMNR program [6]. The values of  $m_c$ ,  $\mu_F/\mu_0$  and  $\mu_R/\mu_0$  were varied similarly to what done by M. Mangano in Ref. [4]. The errors correspond to the curve obtained with the set of parameters used for our baseline cross section:  $m_c = 1.2$  GeV,  $\mu_F/\mu_0 = \mu_R/\mu_0 = 2$  and CTEQ 4M PDFs. The figure shows that the broad ALICE  $p_t$  coverage, from almost zero

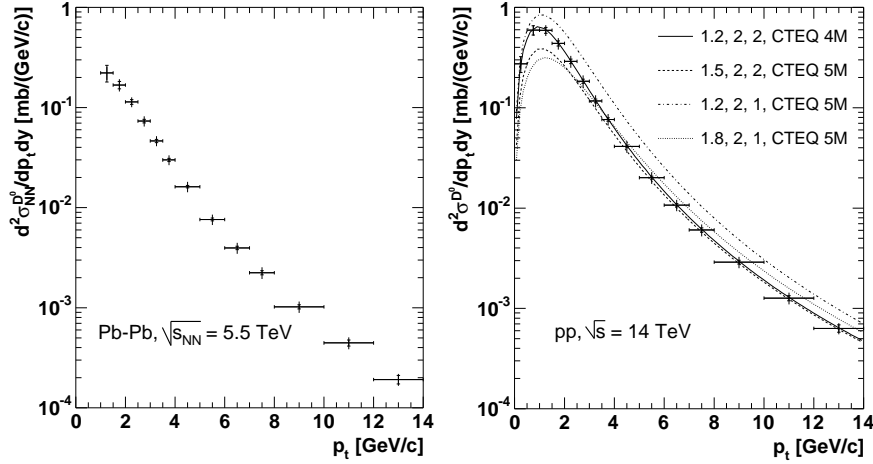


Fig. 2. Differential cross section per NN collision for  $D^0$  production as a function of  $p_t$ , as it can be measured with  $10^7$  central Pb–Pb events (left) and  $10^9$  pp minimum-bias events (right). Statistical (inner bars) and  $p_t$ -dependent systematic errors (outer bars) are shown. A normalization error of 11% for Pb–Pb and 5% for pp is not shown. For pp (right) pQCD predictions obtained with different sets of the input parameters  $m_c$  [GeV],  $\mu_F/\mu_0$ ,  $\mu_R/\mu_0$  ( $\mu_0$  is defined in the text) and PDF set are also reported.

to about 14 GeV/ $c$ , gives a good constraining power with respect to the pQCD input parameters.

#### 4 ALICE sensitivity to D-meson suppression

The D-meson nuclear modification factor  $R_{AA}^D(p_t)$ , defined in Eq. (2), is reported in Fig. 3 (top-left panel). Only nuclear shadowing is included (no energy loss). The reported errors are obtained combining the previously-mentioned errors in Pb–Pb and in pp collisions and considering that several systematic contributions will partially cancel out in the ratio. The uncertainty of about 5% introduced in the extrapolation of the pp results from 14 TeV to 5.5 TeV by pQCD, estimated in Ref. [19], is also shown.

The effect of shadowing, introduced via the EKS98 parameterization [8], is visible as a suppression at low transverse momenta,  $p_t \lesssim 7$  GeV/ $c$ , corresponding to small  $x$  ( $\lesssim 10^{-3}$ ). Since there is a significant uncertainty on the magnitude of shadowing in this  $x$  region, we studied the effect of such uncertainty on  $R_{AA}$  by varying the modification of the PDFs in a Pb nucleus (shown for gluons in top-right panel of Fig. 3). Even in the case of shadowing 50% stronger than in EKS98 (curves labelled “c”), we find  $R_{AA} > 0.93$  for  $p_t > 7$  GeV/ $c$ . We can, thus, conclude that c-quark energy loss can be cleanly studied, being the only expected effect, in the

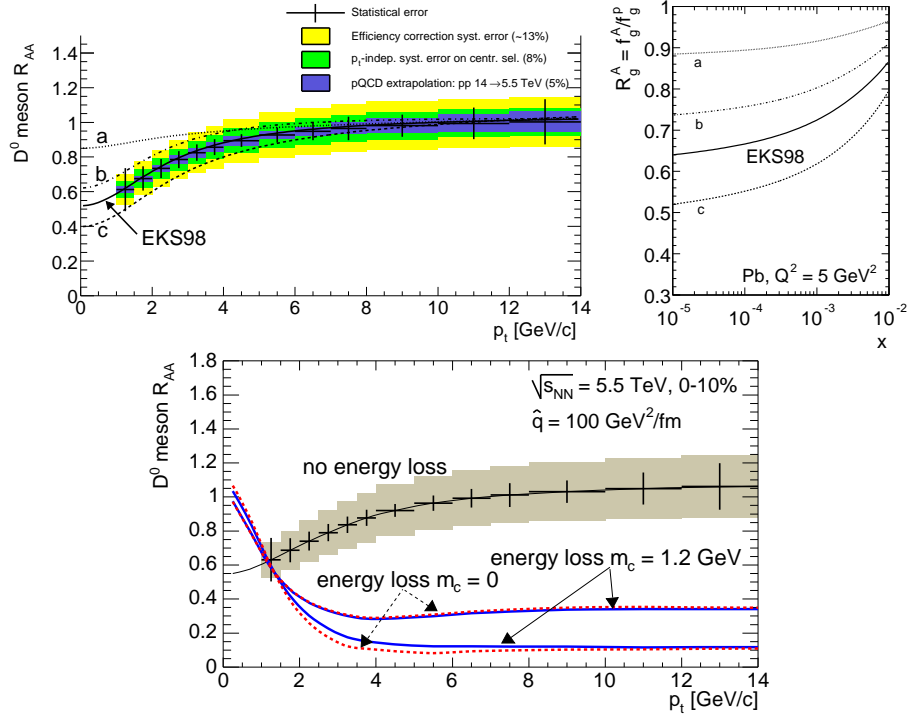


Fig. 3. Top-left:  $R_{AA}$  of  $D^0$  mesons (only shadowing included) with the statistical errors and the different contributions to the systematic error. Top-right: different nuclear modifications of the gluon PDF at the scale  $Q^2 = (2m_c)^2 = 5$  GeV<sup>2</sup>. Bottom:  $R_{AA}$  of  $D^0$  mesons, without energy loss ('data' points), with energy loss for massless quarks ( $m_c = 0$ ; dashed line) and with energy loss for massive quarks ( $m_c = 1.2$  GeV; solid line). The reported errors are: bars = statistical, shaded area = systematic contributions combined.

region  $7 \lesssim p_t \lesssim 15$  GeV/ $c$ , where ALICE has a good sensitivity.

In the bottom panel of Fig. 3 we report a recent estimate of the suppression of the D-meson nuclear modification factor in central Pb–Pb collisions at the LHC [21], obtained in the framework of the PQM model [14], where energy loss is simulated in a parton-by-parton approach combining the BDMPS ‘quenching weights’ [22] and a Glauber-model-based definition of the in-medium parton path length. The quenching weights were specifically calculated for massive partons, using the formalism developed in Ref. [17]. The medium transport coefficient at the LHC was set to the value  $\hat{q} = 100$  GeV<sup>2</sup>/fm, estimated on the basis of the analysis of RHIC data performed in Ref. [14]. The results are plotted as a band that represents the theoretical uncertainty arising from the finite-energy constraint discussed in Section 2. According to this estimate the c-quark mass does not influence the observed

suppression of D mesons in any significant way.

## 5 Conclusions

We have shown that the direct  $D^0$ -meson reconstruction with ALICE will allow to measure the charm cross section in pp collisions and its medium-induced suppression in Pb–Pb collisions, thus providing stringent experimental constraints to the current theoretical understanding both in the domain of perturbative QCD calculations and in that of many-body high-density QCD, where parton energy loss is computed.

Discussions with F. Antinori, E. Quercigh and K. Šafařík are gratefully acknowledged. The author thanks the organizing committee of the conference “Physics at LHC 2004”, where this talk was presented, for supporting his participation.

## References

- [1] ALICE Physics Performance Report, Volume I, CERN/LHCC 2003-049 (2003); C. Fabjan, *these proceedings*.
- [2] B. Muller, *these proceedings*.
- [3] N. Armesto, *these proceedings*.
- [4] M. Bedjidian *et al.*, CERN Yellow Report *in press*, arXiv:hep-ph/0311048.
- [5] N. Carrer and A. Dainese, ALICE-INT-2003-019 (2003), arXiv:hep-ph/0311225.
- [6] M. Mangano, P. Nason and G. Ridolfi, Nucl. Phys. B **373** (1992) 295.
- [7] H.L. Lai *et al.*, CTEQ Coll., Phys. Rev. D **55** (1997) 1280.
- [8] K.J. Eskola, V.J. Kolhinen and C.A. Salgado, Eur. Phys. J. C **9** (1999) 61.
- [9] J. Harris, *these proceedings*.
- [10] M. Gyulassy and X.N. Wang, Nucl. Phys. B **420** (1994) 583.
- [11] R. Baier, Yu.L. Dokshitzer, A.H. Mueller, S. Peigné and D. Schiff, Nucl. Phys. B **483** (1997) 291; *ibidem* B **484** (1997) 265.
- [12] U.A. Wiedemann, Nucl. Phys. B **588** (2000) 303.
- [13] M. Gyulassy, P. Lévai and I. Vitev, Nucl. Phys. B **571** (2000) 197; Phys. Rev. Lett. **85** (2000) 5535; Nucl. Phys. B **594** (2001) 371.
- [14] A. Dainese, C. Loizides and G. Paic, arXiv:hep-ph/0406201.
- [15] Yu.L. Dokshitzer, V.A. Khoze and S.I. Troyan, J. Phys. G **17** (1991) 1602.
- [16] Yu.L. Dokshitzer and D.E. Kharzeev, Phys. Lett. B **519** (2001) 199.
- [17] N. Armesto, C.A. Salgado and U.A. Wiedemann, Phys. Rev. D **69** (2004) 114003.
- [18] N. Carrer, A. Dainese and R. Turrisi, J. Phys. G **29** (2003) 575.
- [19] A. Dainese, Ph.D. Thesis, arXiv:nucl-ex/0311004.
- [20] T. Sjöstrand *et al.*, Computer Phys. Commun. **135** (2001) 238.
- [21] N. Armesto, A. Dainese, C.A. Salgado and U.A. Wiedemann, *in preparation*.
- [22] C.A. Salgado and U.A. Wiedemann, Phys. Rev. D **68** (2003) 014008.